Computers and Concrete, *Vol. 25, No. 1* (*2020*) *15-27*
DOI: https://doi.org/10.12989/cac.2020.25.1.015

Monitoring of fracture propagation in brittle materials using acoustic emission techniques-A review

Hamid Reza Nejati*[1], Amin Nazerigivi[1], Mehrdad Imani[1] and Ali Karrech[2]

[1]*Rock Mechanics Division, School of Engineering, Tarbiat Modares University, Tehran, Iran*
[2]*School of Civil, Environmental and Mining Engineering, Faculty of Engineering, Computing and Mathematics, The University of Western Australia, Australia*

(*Received November 9, 2018, Revised October 1, 2019, Accepted January 4, 2020*)

Abstract. During the past decades, the application of acoustic emission techniques (AET) through the diagnosis and monitoring of the fracture process in materials has been attracting considerable attention. AET proved to be operative among the other non-destructive testing methods for various reasons including their practicality and cost-effectiveness. Concrete and rock structures often demand thorough and real-time assessment to predict and prevent their damage nucleation and evolution. This paper presents an overview of the work carried out on the use of AE as a monitoring technique to form a comprehensive insight into its potential application in brittle materials. Reported properties in this study are crack growth behavior, localization, damage evolution, dynamic character and structures monitoring. This literature review provides practicing engineers and researchers with the main AE procedures to follow when examining the possibility of failure in civil/resource structures that rely on brittle materials.

Keywords: fracture process; acoustic emission; brittleness; damage evolution; failure modes

1. Introduction

Acoustic emission techniques (AET) is unique among non-destructive testing methods (NDT) in the sense that it is typically applied during the loading process unlike other NDT methods that are applied before or after the loading of a structure. Furthermore, AET is regularly used to identify defects at early stages before catastrophic failures take place (Grosse and Ohtsu 2008).

Like in seismology where mechanical waves collected in stations located on the earth surface and processed to determine the source and magnitude of a tremor, data about the presence and location of potential failure sources are collected and analyzed. In AET, transient elastic waves are produced by the prompt release of energy from localized sources within a material. This phenomenon could be based upon both the generation and propagation of flaws. Therefore, elastic waves moving through the solid surface are detected by sensors, which convert the mechanical waves into electrical signals (Chakrabarti and Benguigui 1997, Carpinteri *et al*. 2007).

A typical AE signal is depicted in Fig. 1, which indicates key parameters such as counts, amplitude, duration, rise time, and threshold. These parameters are described as follows (Nazerigivi *et al*. 2017):

Threshold: the operator assumed value of amplitude in decibels (dB), normally decided and set based on background noise.

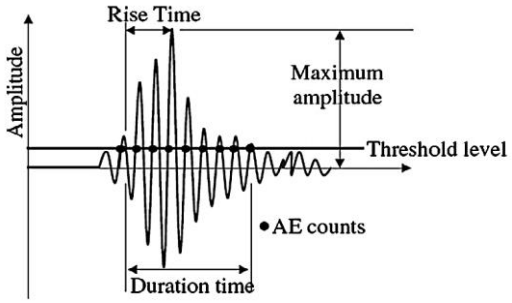

Fig. 1 Typical AE signal and parameters (Aggelis 2011)

Hit: a signal that surpasses the threshold and results a system channel to gather data.

AE counts: Number of times that an AE signal surpasses a distinct threshold during one AE signal.

Amplitude: the maximum value of the AE signal and usually expressed in decibels.

AE energy: the space under the amplitude-time curve above the threshold value.

Rise-time: related to the time interval starting from the time of AE signal generation to the time of the signal achieving its maximum amplitude.

AE duration: states the time span from the starting point to the end point of the AE signal.

Moreover, two useful parameters that can be deduced indirectly based on AE signal are known as the Raise Angle (RA) and Average Frequency (AF). These parameters are calculated from rise time divided by amplitude and count divided by duration, respectively (Aggelis 2011).

RA value=rise time/maximum amplitude;

Average Frequency=AE counts/duration

*Corresponding author, Ph.D.
E-mail: h.nejati@modares.ac.ir

ISSN: 1598-8198 (Print), 1598-818X (Online)

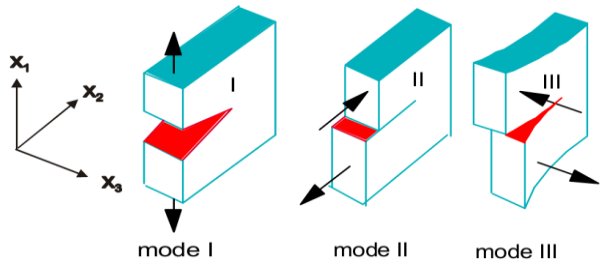

Fig. 2 Failure modes: (I) mode I or opening mode, (II) mode II or sliding mode, (III) mode III or the tearing mode (Kumar and Barai 2011)

By the early 1960s, this method was employed in the USA to examine the integrity of pressure vessels. Many attempts had been made to decipher the significance of AET in monitoring the performance of metals during deformation and fracture. Kaiser (1950) conducted an investigation on metals in Germany and discovered a distinguished feature, which is called Kaiser effect. He revealed that in a simple cyclic loading the AE activity is zero or trivial like the background level when uniaxial loading by the cycle's peak stress rising from cycle to cycle considering the stress endures lower than the major formerly gained stress value. In this case, the AE activity increases intensely once this peak stress value is touched (Lavrov 2003).

Other studies (Blake and Leighton 1969, Blake 1972) were reported by the U.S. Bureau of Mines in Idaho in deep coal mines (up to 1000 m) and additional details about geotechnical field applications were revealed. The deformation and fracture behavior of diverse materials such as medium carbon steel and austenitic alloys have been studied by AE technique and an enriched insight into correlations among the frequency, amplitude, and tensile deformation have been made (Raj and Jayakumar 1991, Mukhopadhyay *et al*. 2010, Haneef *et al*. 2010). Other early researchers have focused their interest on concrete (Rüsch 1960, L'Hermite 1960, Robinson 1965) and the most significant use of AET to concrete structures commenced in the late 1970s (Carpinteri *et al*. 2007). Once the novel technology advanced further for it was adjusted to investigate the behavior of heterogeneous materials (Carpinteri *et al*. 2007).

2. Fracture mechanics of brittle materials

The behavior of materials in the neighborhood of a crack and at the crack tip is the subject of fracture mechanics. Quasi-brittle materials such as cementitious materials, rocks, and fiber-reinforced composites typically contain defects in their intrinsic matrices. The shear surfaces, cracks, weak surfaces and fault ages (in rock) and pores in cement, cracks at matrix-aggregate interface, and shrinkage cracking (in composite materials) have important impact on the mechanical behavior of structures at various scales (Kumar and Barai 2011). Failure of concrete or rock structures is usually accompanied by expansion of interior cracks due to stress concentration at the cracks tip

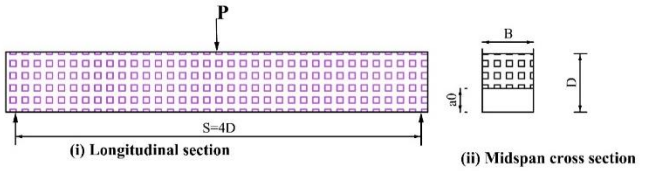

Fig. 3 The geometry of TPBT (Kumar and Barai 2011)

(Nazerigivi *et al*. 2018). The pioneering development of fracture mechanics is often attributed to Inglis in 1913 who modeled a crack-like discontinuity as elliptical hole in an infinite linear elastic plate loaded at its exterior boundaries to analyze stresses. Then, in 1921, Griffith presented a new energy-based failure criterion to define the first description of the mechanism of brittle fracture (Kumar and Barai 2011).

Moreover, researchers have developed some mathematical procedures to describe the distribution of stress near a crack tip and revealed that the stress field is quasi-singular near a crack tip. It also reduces in proportion to the square root of the distance to the crack tip r ($r \ll a$, and a is the crack length) (Irwin 1957). Also, three types of different failure modes such as mode I, mode II, and mode III are shown in Fig. 2 (Whittaker *et al*. 1992).

Varied test procedures to determine fracture parameters have been introduced based on different standards. While carrying out direct methods like uniaxial tensile test with displacement controlled is difficult, using indirect methods with several geometrical shapes has been commonly expanded to determine the fracture parameters. These common indirect methods are three-point bending test (TPBT), compact tension (CT) test, and wedge splitting test (WST) as follows (Kumar and Barai 2011):

2.1 Three-Point Bending Test (TPBT)

TPBT is one of the most suitable geometries to examine the physical parameters that are required in different fracture models. The recommendations for calculating the fracture energy of cementitious materials can be found in RILEM Technical Committee 50-FMC (1985). Also, the crack mouth opening displacement (CMOD) and crack tip opening displacement (CTOD) can be measured by this test method (Zhang *et al*. 2013, Zhang *et al*. 2015, Zhang *et al*. 2016). Fig. 3 shows the standard dimensions of the TPBT where the symbols $a0$, B, D, and S are the notch size, beam width, beam depth, and loading span, respectively. In the case of TPBT, the span to depth ratio is usually S/D=4 and the crack notch is positioned halfway through the span.

2.2 Compact Tension (CT) test

The standard CT consists of a single-edge notched plate subjected to a tension load as explained in the ASTM Standard E-399. The dimensions and configuration of a standard CT specimen are given in Fig. 4 indicating that the dimensions should verify Dt=1.25D, H=0.6D, $H1$=0.275D, and the specimen thickness B=0.5D. It can be seen that the sides of sample are almost twice the specimen thickness and during the test load and deformation are detailed and finally

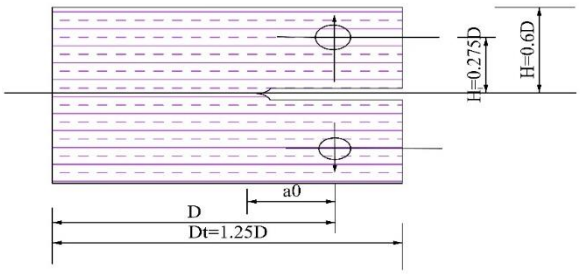

Fig. 4 The geometry of CT (Kumar and Barai 2011)

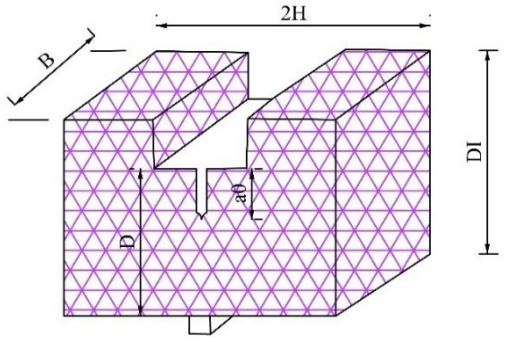

Fig. 5 Dimensions of WST (Kumar and Barai 2011)

crack length is measured on the fractured test part.

2.3 Wedge Splitting Test (WST)

The WST consists of two immense steel-loading plans fortified with roller bearings on each side of the specimen. Fracture toughness and specific fracture energy are the main two factors which can be measured by this method by means of specimens like cubes or cylinders. Once a notched specimen is set on a linear support, two loading devices provided with rollers are applied on the top of the specimen (Brühwiler and Wittmann 1990). The general shape and dimensions of commonly used WST specimen are shown in Fig. 5.

Several other testing methods to determine fracture parameters of rocks have been developed. ISRM has proposed Short rod specimen method (SR), Chevron bend specimen method (CB) and Cracked Chevron Notched Brazilian Disc method (CCNBD) in the filed or rock engineering (Franklin *et al.* 1988, Fowell *et al.* 1995). Szendi-Horvath (1982) introduced diametrical compression methods to investigate fracture toughness of coal. Since these testing methods are relatively simple both in preparation and calculation of fracture parameters, they are common in practice. Two of these methods, namely the Single-edge Cracked Brazilian Disks (SECBD) and the Central Straight-through Crack Brazilian Disk (CSCBD) are summarized in this section (Sabri *et al.* 2016).

2.4 Single-edge Cracked Brazilian Disks (SECBD)

SECBD has a straight notch cut along the diameter on one face. This type of specimens has been used for indirect tension tests. A schematic representation of SECBD specimens is shown in Fig. 6.

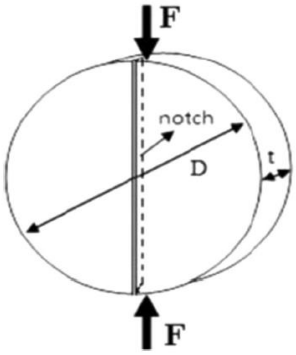

Fig. 6 The standard geometry of SECBD (Whittaker *et al.* 1992)

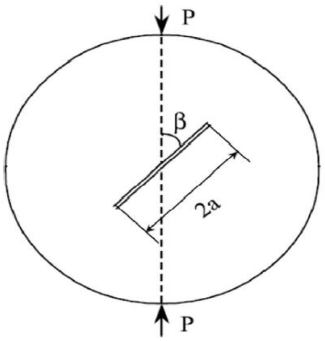

Fig. 7 The standard geometry of CSCBD (Sabri *et al.* 2016)

The fracture toughness can be calculated by using the following equation (Szendi-Horvath 1982)

$$K_I = \frac{1.264P\sqrt{a}}{BD} \quad (1)$$

where K_I [Pa $m^{0.5}$] is the fracture toughness, P [N] is compressive load at yielding, a [m] is notch depth, D [m], and B [m] are diameter and thickness of the disk, respectively.

2.5 Central Straight-through Crack Brazilian Disk (CSCBD)

CSCBD method is the most famous analysis technique for determination of fracture toughness in modes I, II and I-II in rock samples. The fracture toughness is assessed by compressing a standard disc with central crack inclined by an angle of β with respect to the loading axis as shown in Fig. 7 (Sabri *et al.* 2016).

It should be mentioned that a critical idiom and following equations which have been adopted from Atkinson *et al.* (1982) and utilized to calculate the fracture toughness of concrete based on CSCBD specimens

$$K_I = \frac{P\sqrt{a}}{\sqrt{\pi}RB} N_I \quad (2)$$

$$K_{II} = \frac{P\sqrt{a}}{\sqrt{\pi}RB} N_{II} \quad (3)$$

where K_I is mode I stress intensity factor, K_{II} is mode II stress intensity factor, R is the radius of Brazilian disk, B is

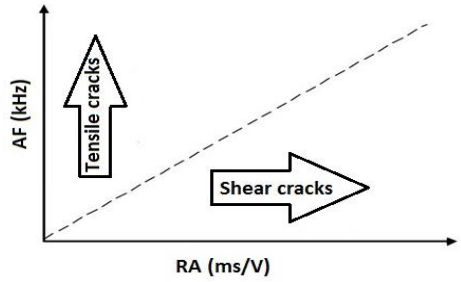

Fig. 8 Classification of crack type with arrangement of AF and RA values (Nazerigivi *et al*. 2017)

thickness of the disk, P is compressive load at failure, a is half crack length, N_{I} and N_{II} are non-dimensional coefficients which depend on ratio of half crack to radius (a/R) and crack orientation angles with respect to the diametrical load. They also proposed the following equations to determine the terms N_{I} and N_{II} of relatively small crack length ($a/R \leq 0.3$) (Atkinson *et al.* 1982)

$$\mathrm{N_I} = 1 - 4\sin^2\beta + 4\sin^2\beta\,(1 - 4\cos^2\beta)\left(\frac{a}{R}\right)^2 \quad (4)$$

$$\mathrm{N_{II}} = [2 + (8\cos^2\beta - 5)\left(\frac{a}{R}\right)^2]\sin 2\beta \quad (5)$$

2.6 Clarification of failure modes by AET

The most significant aim of acoustic emission monitoring is to collate AE signals through developing fracture process or deterioration to prevent catastrophic fails in structures by establishing rational correlations among AE parameters which were discussed in introduction section (Grosse and Ohtsu 2008).

Researchers have been conducting many investigations to clarify failure modes in brittle materials. The standard classification of crack types in concrete materials proposed by JCMS (2003) is based upon the combination of the average frequency and the RA values as can be seen in Fig. 8. It was observed that in the process of fracture, AE generations in the early stage show higher AF and lower RA, however, at final stage RA value increases in comparison to AF (Grosse and Ohtsu 2008).

Moreover, for rock materials 'grade' parameter was suggested (Shiotani *et al*. 2001). It is defined as an incline of a mounting part of AE waveform in rock materials. Like RA/AF correlation, at early stage tensile cracks would be mainly detected, then shear type of cracks would be dominated at final stage. Therefore, the incline of the mounting part in the waveform reduces as the fracture progresses (Shiotani *et al*. 2001).

3. Detection and evaluation of crack growth behaviour

Since perceiving the behavior and mechanism of crack coalescence thoroughly in brittle materials such as rock and concrete is highly complicated, crack growth is known to be extremely complex. Crack propagation in concrete and rocks are inherently uncertain in comparison to crack propagation in homogenous materials such as glass, due to their intricate matrix-including various fiber composites, additives, aggregate particle sizes. In brittle materials, a recognized area ahead of the crack tip can be sensed during crack propagation, which is identified as fracture process zone (FPZ) (Ohtsu 2015). Unlike in ductile materials where the FPZ is quite small and can be ignored, brittle materials exhibit relatively large FPZ. Hence, linear elastic fracture mechanics (LEFM) can be applied in the case of ductile materials, but fails to capture the complexity of brittle ones. For example, in concrete and rocks, the nonlinear zone at the crack tip is fully dominated by FPZ and applying of LEFM is uncommon. Yet, it is vital to predict crack growth in heterogeneous and anisotropic materials such as rocks and concrete to predict their performance in engineering structures (Ohtsu 2015, Kumar and Barai 2011).

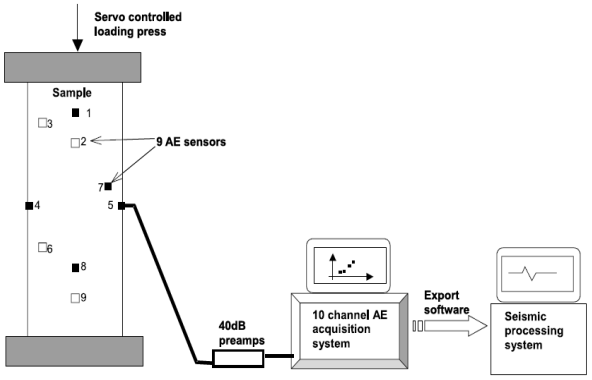

Fig. 9 The installation of AE sensors and test procedure (Sellers *et al*. 2003)

3.1 Localization procedure and FPZ

There are several methods to localize the sources of AE signals in experimental programs, which are mainly based on application, material properties and specimen geometry. The source location of flaws can be estimated by using the commencement time of fracture recorded by each sensor. The fundamental examples of localization by AET can be found in (Zang *et al.* 1998, Ohtsu 1998, Köppel and Grosse 2000, Sellers *et al*. 2003, Kurz and Grosse 2005).

Sellers *et al*. (2003) used a series of uniaxial compression tests on 96-mm-diameter and 242-mm-length quartzite samples to investigate the scaling of rock fracture process and source localization. They attached 9 AE sensors to each sample to monitor AE events as can be seen in Fig. 9. They stated that in the early steps of loading AE, events were spread all over the specimens and then at final steps became in line on planes. Moreover, a new hybrid relative moment tensor analysis which removes the impact of unknown sensor-coupling coefficients and path influences was applied and revealed that events in each group of examination showed the same propagation path to the recording stations. Thus, observed failure planes were mostly similar to later event locations and anticipated central planes.

It was concluded that there are correlations among FPZ,

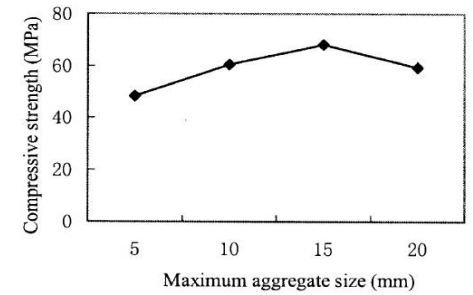

(a)

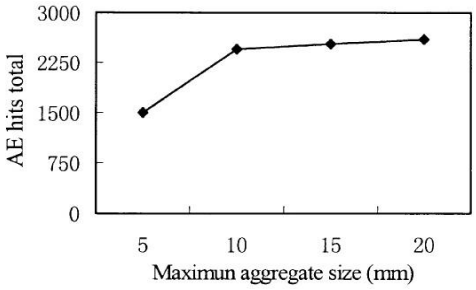

(b)

Fig. 10 The correlation between (a) compressive strength and (b) AE total hits with different content of aggregate size (Wu *et al*. 2001)

aggregate size, and the sample size in concrete. The results showed that the growth of FPZ has a direct influence on the increase in the aggregate size. Moreover, it was reported that specimens with larger aggregate size produce more fracture energy (Ohno 2015).

Based on the discussion above, there is a sensible correlation between FPZ and source location in AE technique since the process of fracture can be determined by variety in arrival time of AE events, location of AE sensors, and P-wave velocity (Grégoire *et al*. 2015). Haidar *et al*. (2005) used a model mortar material to investigate the correlation among the width of the FPZ calculated by AET analysis, size effect parameters, and the internal length of flaw. A practical rough calculation of the internal length estimated by experimental AE localization tests can be provided by this correlation.

Grégoire *et al*. (2015) conducted numerical and experimental studies to evaluate FPZ using acoustic emission. The experimental program showed a good agreement with numerical approach especially in terms of distances between damage zones and timing of damage events. The results indicated that the calculated acoustic energy is highly correlated with the energy dissipated due to failure.

3.2 Particle size effects

As in composite materials aggregates represent about 70% the total volume, they play an important role in the overall performance. Several studies have focused on the correlations among fracture parameters and aggregates size (Wittmann 1986, Mihashi *et al*. 1991).

Wu *et al*. (2001) reported the influence of aggregate size distribution on the mechanical properties of concrete. They

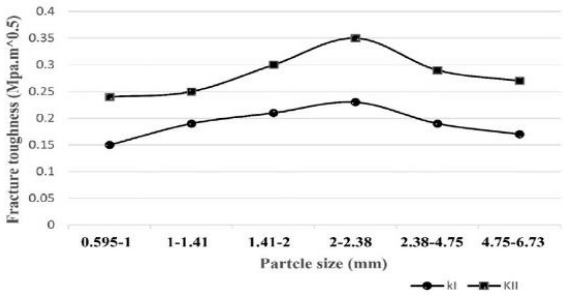

Fig. 11 Variation of KI and KII failure modes with different grain particle sizes (Sabri *et al*. 2016)

used uniaxial compression and three-point-bending tests to provide correlations among maximum aggregate size, compressive strain, and fracture energies by means of acoustic emission. They concluded that the compressive strength of concrete improves by increasing the aggregate size up to level 15 mm then reduces as can be seen in Fig. 10(a). On the other hand, AE cumulative hits increase with the maximum aggregate size as shown in Fig. 10(b).

Other researchers such Watanabe *et al*. (2007) as worked on the compressive failure of concrete embedding recycled aggregates. They declared that nucleation of tensile and shear cracks during loading sequence was different in both concretes (normal concrete and concrete of recycled aggregate). Moreover, micro-cracking which was observed by AE hits can be reduced considerably through vibration after mixing and micro-cracking in concrete sample of recycled aggregate can be sensed at lower stress level than normal concrete samples.

The effect of grain size on the failure mechanisms and toughness of rocks and rock-like materials was investigated by Sabri *et al*. (2016). To this end, several Single-Edge Cracked Brazilian Disks (SECBD) Granite specimen and Central Straight-through Crack Brazilian Disk (CSCBD) rock-like specimens were prepared. As shown in Fig. 11, the fracture toughness obtained for modes II and I is indirectly related to particle size. However, the specimens with medium grain size (2-3 mm) hold the maximum fracture toughness in both test series.

3.3 Reinforced concrete

Acoustic emission characterization of the failure mechanism varies in different types of fibers in concrete matrix (Najigivi *et al*. 2017). Aggelis *et al*. (2011) showed that the severe changes in average frequency can be sensed during fiber pull out contributing in shifting failure mechanism from tensile micro cracking to macro cracking. On the other hand, the number of hits and the fiber content exposed a nearly linear relation. Because each fiber pull out event is a possible AE hit and the pull out events rise with the fiber volume content (Soulioti *et al*. 2009).

Moreover, AET was applied successfully to monitor fracture energy of fiber reinforced polymer concrete. Chopped glass fibers were used in notched beams according to RILEM (Carpinteri and Shah 2014) to investigate the fracture parameters. The acoustic emission energy can be calculated by Eq. (6) (Reis *et al*. 2003)

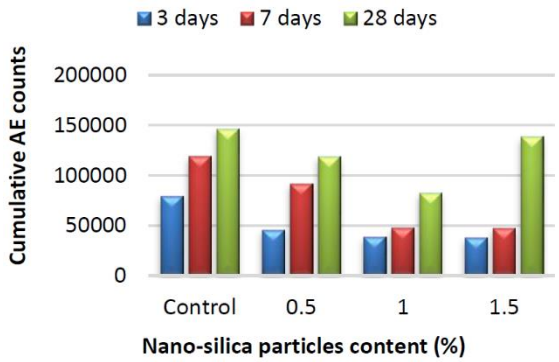

Fig. 13 Cumulative AE counts during compressive load for both types of cement mortar specimen at different age of tests (Nazerigivi *et al*. 2017)

$$E_{AE} = \int_{0}^{t_{ae}} [V(t)]^2 dt \quad (6)$$

where $V(t)$ and t_{ae} are the recorded AE transient voltage signal and the duration of the event, respectively.

It was concluded that AET can be used effectively in the case of polyester-polymer concrete because of their high brittle nature in which high fracture energy released and converted to acoustic energy. Furthermore, fracture energy activity showed a gradual increase up to peak load and then a rapid increase indicating major structural degradation. This behavior can be confirmed by the slight propagation of cracks before yielding followed by crack localization and rapid material softening as shown in loading curve generating the FPZ (Reis *et al*. 2003).

Other researchers worked on chemical admixtures in concrete to monitor fracture process. Haneef *et al*. (2013) studied the influence of fly ash and curing on crack growth in concrete during uniaxial compression testing using acoustic emission (AE) technique. They stated three different stages for cracking in concrete, namely crack closure/micro-cracking, steady crack propagation and unstable crack propagation. Besides, the results showed that the addition of fly ash to concrete matrix can modify the stress and strain of samples without unstable crack propagation.

Furthermore, Nazerigivi *et al*. (2018) investigated the effects of SiO_2 nanoparticles on failure mechanism of binary blended concrete by AET. In addition, they examined the pure mode I (tension) and pure mode II (shear) in concrete samples. As can be seen in Fig. 12, the RA distributions of both concrete types vary with different amounts of Nano-SiO_2 (0% or control, 0.2%, 0.5%, and 0.8%) and binary blended concrete has higher RA values than control concrete. The higher RA value of binary blended concrete indicated that the shear cracks are more than the tensile cracks at all the diverse contents of nano blended concrete samples.

Moreover, the AE counts during compression loading varied depending on the curing days and SiO_2 content nanoparticles in mortar specimens. Fig. 13 shows that the variation of cumulative AE counts through compressive loading of specimens with SiO_2 nanoparticles reduced as

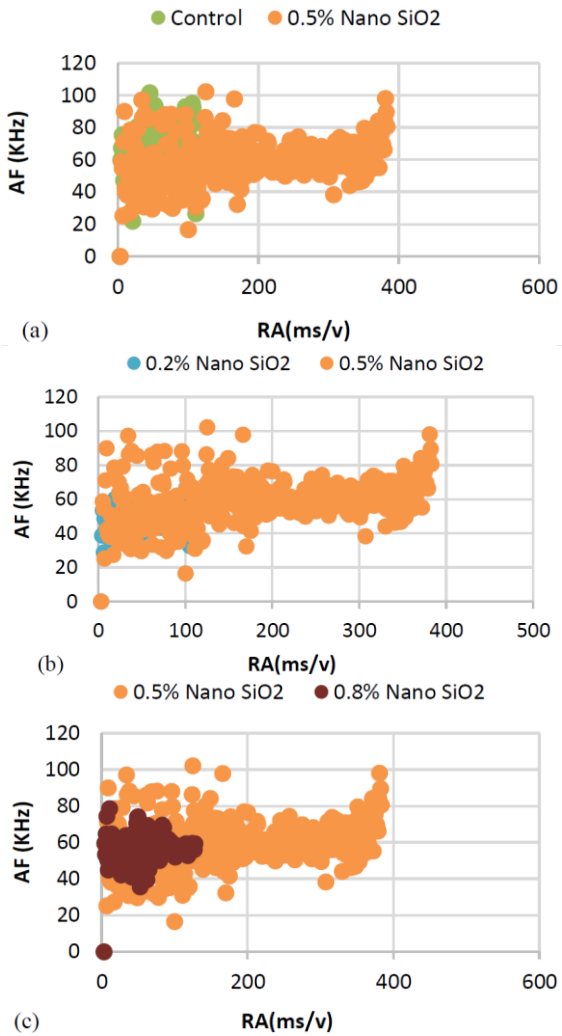

Fig. 12 Variation of AF with RA (a) control concrete and concrete with 0.5% Nano SiO_2 (b) concrete with 0.2% and 0.5% Nano SiO_2 (c) concrete with 0.5% and 0.8% Nano SiO_2 (Nazerigivi *et al*. 2018)

compared to the control specimens for entirely ages of curing period (Nazerigivi *et al*. 2017, Nazerigivi *et al*. 2019).

3.4 Other aspects of studies

Several other scholars have worked on different and special aspects of AET investigation of brittle materials. The behavior of concrete under different moisture contents was studied by Ranjith *et al*. (2008). They used dry, partially wet and fully wet concrete specimens to this end. The effect of water on AE events can be seen in Fig. 14. The increase of moisture content in concrete specimens has reduced the AE counts considerably. It was concluded that water content can alter the crack sensitivity in concrete matrix.

Moreover, Dzaye *et al*. (2018) studied the characterization of AE events in fresh concrete by examining the aggregate and bubble movement. The arrangement of sensors in a standard mold of fresh concrete can be seen in Fig. 15. The results demonstrate that only

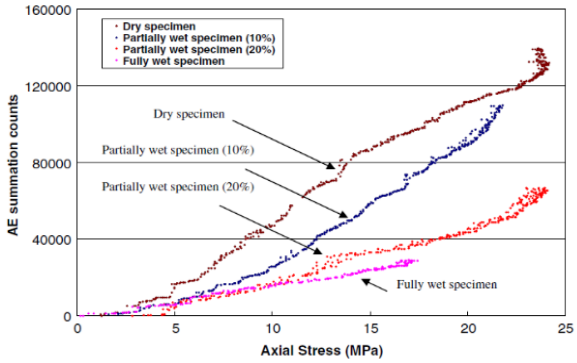

Fig. 14 Variation of AE event counts through different moisture contents (Ranjith *et al*. 2008)

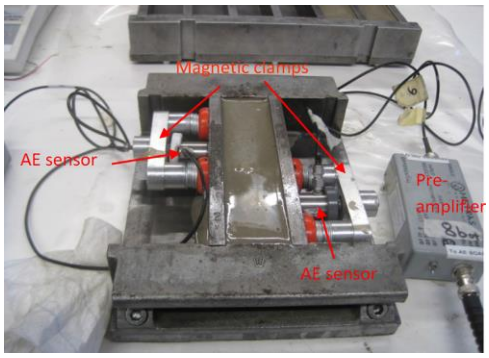

Fig. 15 The arrangement of AE sensors at fresh concrete mold (Dzaye *et al*. 2018)

mechanical sources situated near the mold in fresh paste may generate a strong elastic wave in spite of some other sources. Hence noticeable AE events over the liquid matrix can be due to aggregates motion because of settlement, separation and formation/motion of bubbles.

As AE activities can be sensible to corrosion of reinforcing steel bars, AET is a valuable method to monitor the process of corrosion in rebar. There are several researches in this field (Kawasaki *et al*. 2011, Ohtsu *et al*. 2011, Kawasaki *et al*. 2015).

Ohtsu *et al*. (2011) conducted a project on AE monitoring of reinforced concrete sample subjected to an accelerated corrosion process. It is worth mentioning that the corrosion process can be divided into 4 phases based on corrosion loss and time (hours); the creation of corrosion is at phase 1, the rate of the corrosion loss declines at phase 2 since the flow of oxygen is considerably impeded, and lastly at phases 3 and 4 more corrosion loss occurs because of anaerobic corrosion. They suggested that the start of corrosion commenced after 48 hours and after 72 to 96 hours, a sudden reduction in the average frequency could be noticeable. Thus, because of the beginning of corrosion in rebar, cracks other than tensile cracks are generated. Comparing all different periods, large-scale tensile cracks were powerfully nucleated about 288 h period.

Numerous experimental and numerical approaches were undertaken in order to evaluate the crack path, mix mode fracture toughness, and influence of crack length in rocklike materials of low brittleness. They used CSCBD method as mentioned previously in order to conduct the project. The

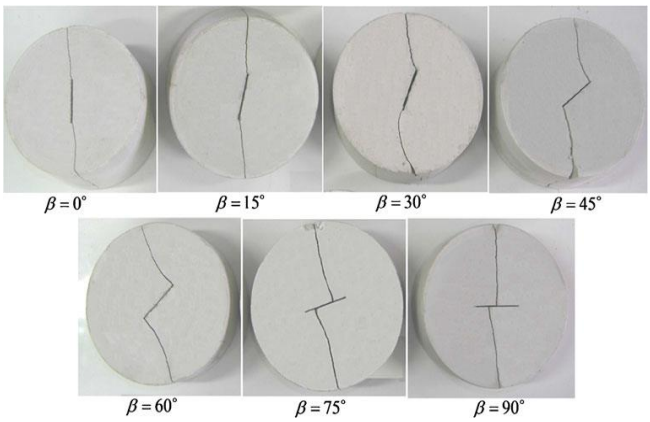

Fig. 16 Experimental modeling result (a/R=0.3), failure mode of rock-like material specimen for different inclination angles (Ghazvinian *et al*. 2013)

results indicated that for specimens with values of $\beta \leq 60°$ the central crack has propagated at the tip of the flaw. In contrast, for specimens with $\beta \geq 75°$ the crack has not propagated from the flaw tip (Fig. 16). In other word, growth of existing flaw caused the specimens failure at $\beta \leq 60°$ while the specimens at $\beta \geq 75°$ failed in a tensile splitting mode. They also suggested that the existence of flaw did not have impact on the specimen failure when the inclination angle is equal or more than 75° since mode I intensity stress factor in the crack tips decreased (Ghazvinian *et al*. 2013).

Furthermore, Hall *et al*. (2006) used a combination of acoustic emission and digital images to monitor fracturing in a soft rock (Neapolitan Tuff). It was concluded that failure of Neapolitan fine-grained tuff in the presence of pre-existing cracks depends on the closeness of the cracks. However, a conventional explanation of failure for samples without pre-existing or only one crack suggests three distinct stages (crack closure, stable crack growth, and unstable crack growth) but for samples with two pre-existing cracks, the third stage can be separated into two parts as failure occurs merely after both the unstable propagation of external wing cracks and coalescence of the internal cracks. Subsequently, AE signatures were the only potential detector to determine the timing in failure, while progress of fracture geometry can be described by the photographs.

4. Damage evolution

The assessment of safety and durability for concrete structures, like lining of tunnels, bridges and viaducts or masonry historical buildings demands intricate considerations. Since the reliability and failure mechanisms in these structures are often influenced by harsh environments, such as high and inconstant humidity, temperature, chloride, sulphate, and/or acidic fluids (Carpinteri *et al*. 2007, Hadigheh *et al*. 2017). The acoustic emission technique among other diagnoses and monitoring techniques can be valuable (Grosse and Ohtsu 2008, Carpinteri *et al*. 2007).

The scattering of micro-cracks and their evolution results in the damage of brittle materials (Ren *et al*. 2011). The damage evolution and accordingly macroscopic behavior of materials would particularly be affected by the nucleation and propagation of micro-cracks. *AE* generation through a loading sequence makes it potential to monitor and analyze the nucleation and evolution of stress-induced cracks. The scale of fracture can be classified by the amplitude. A large number of acoustic signals with small amplitude emit from micro scale fractures, while macro scale fractures, compared to the micro ones, generate less number of events with higher amplitude (Aggelis *et al*. 2011, Nejati and Ghazvinian 2014).

At the geological scale, the correlation between the magnitude and total number of earthquakes is represented by Gutenberg-Richter (*G-R*) law that reads (Gutenberg 2013)

$$\log_{10}(N) = a - bM \tag{7}$$

where a and b are constants, and b is termed as the "*b*-value", M is the magnitude, and N is the total of earthquakes that occur in a precise time window with magnitudes larger than M. It is concluded that the qualified profusion of small to large seismic events can be called as the *b*-value known as the tectonic characteristic (Nejati and Ghazvinian 2014).

The *G-R* relationship between cumulative frequency and magnitude in the case of AET is shown as follows (Nejati and Ghazvinian 2014)

$$\log_{10}(N) = a - b(\frac{A_{dB}}{20}) \tag{8}$$

where A_{dB} is amplitude of *AE* in *dB*, and N is the number of *AE* hits or events with amplitude greater than A_{dB}. The parameter of the *b*-value in Eq. (8) shows the ratio of micro- to macro-crack frequency occurring in a specific loading sequence (Nejati and Ghazvinian 2014, Kurz *et al*. 2006).

With the purpose of evaluation the influence of rock brittleness on fatigue behavior of rocks, a series of experimental investigations was conducted on three rock types with different brittleness: (1) onyx marble as a high brittle rock with almost no plastic deformation, (2) sandstone as a semi-brittle rock with small plastic deformation and (3) soft limestone as a low brittle rock with a large plastic deformation (Nejati and Ghazvinian 2014).

The cumulative distribution of *AE* peak amplitude exhibited by the tested samples of these three rock types can be seen in Fig. 17. The slope of the lines represent the *b*-value of these three types of rocks. It can be seen that soft limestone has a *b*-value of 1.45 while the *b*-values of sandstone and onyx marble are 0.88 and 0.65, respectively. It can be concluded that during a loading sequence, a highly brittle rock generates highly energetic fractures compared to a low brittle rock (Nejati and Ghazvinian 2014).

Suzuki *et al*. (2017) investigated the damage of reinforced concrete to examine the influence of freeze and thaw processes by *AE* and *X*-ray CT. To this end, they studied the relation between the roughness parameter (*Ci*) and the rate (β). The roundness parameter (*Ci*) was introduced to make the geometric parameters measurable and can be estimated as follows

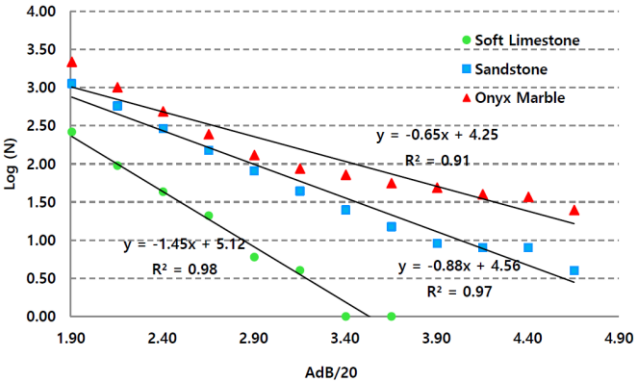

Fig. 17 Cumulative distribution of AE peak amplitude of three different types of rock (Nejati and Ghazvinian 2014)

$$C_i = \frac{P^2}{A} \tag{9}$$

where A (m^2) is the ratio of the area of cracking damage and P (m) are these outer periphery length.

Moreover, the correlation between the probability density function and the strain was illustrated by the rate (β). The tested concrete sample might be damaged in the case that the rate β is negative exhibiting the probability of AE events is high at a low strain level. In contrast, the tested concrete sample is in stable condition in the case that the rate is positive which means the probability is low at low strain level (Suzuki *et al*. 2017).

It was concluded that the level of damage in concrete can be qualitative by *AE* signals since the propagation of the micro-cracks inner concrete affected the reduction in β rate and enlargement of *Ci* (Suzuki *et al*. 2017).

Furthermore, the effects of the sand/cement ratio (1 to 4) on the mechanisms of damage and the fracture process were observed in mortar samples during compressive loading using *AET* and *X*-ray tomography. They concluded that the number of *AE* events increases considerably with the sand to cement ratio, which suggests that the sand to cement boundaries are the favorable location of the *AE* sites (Elaqra *et al*. 2007).

Also, they stated that the pores closing, pore interconnection, multiple crack dividing and sand to cement boundaries cracking are closely associated with the damage level in mortar material (Elaqra *et al*. 2007).

Khodayar and Nejati *et al*. (2018) investigated the effect of thermal-induced micro-cracks on the damage evolution of rock samples. Some of the prepared granite samples were kept in room temperature and the others were heated by a laboratory furnace to different temperature levels (200, 400, 600, 800 and 1000 degree Celsius). Some thin sections of the scanning electron microscope (SEM) induced micro-fractures heated to 800°C and 1000°C and room temperature are shown in Fig. 18.

The number of *AE* hits and amplitude are shown in Fig. 19. It can be seen that the number of *AE* hits generated in the specimen kept at room temperature is more than the number of *AE* hits of heated specimens. Khodayar and Nejati concluded that the frequency of induced fracture under monotonic loading in intact specimen is more than

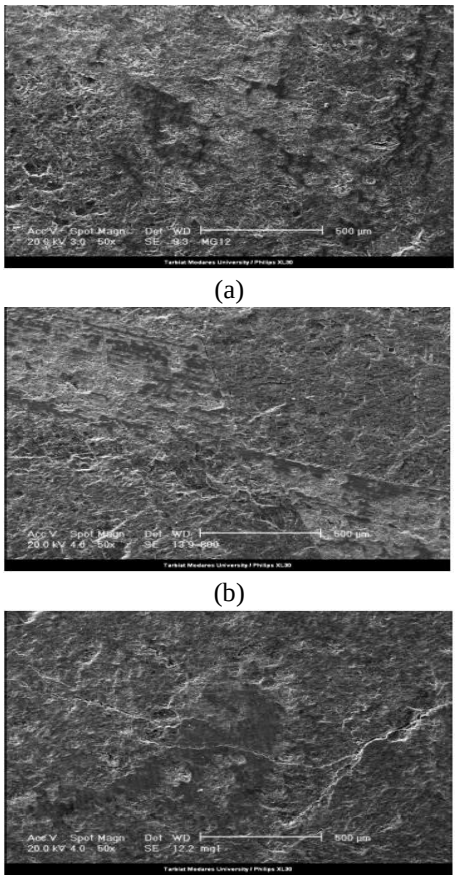

(a) (b) (c)

Fig. 18 SEM images of granite: thin sections (a) at room temperature, (b) heated to 800° C, (c) heated to 1000° C (Khodayar and Nejati *et al*. 2018)

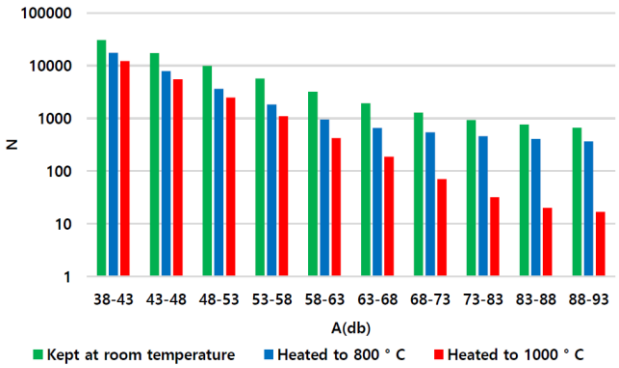

Fig. 19 Variation of number of AE hits with amplitude (Khodayar and Nejati *et al*. 2018)

that in specimens fractured by heating (Khodayar and Nejati *et al*. 2018).

4.1 Dynamic characterization

The dynamic mechanical characteristics of concrete and rocks exposed to high-rate loading needs are different from their static counterparts and often require more complex analysis (Imani *et al*. 2017). A series of experimental tests have been conducted to evaluate the damage of reinforced concrete (RC) beams subjected to incremental cyclic loading. The AE data analysis revealed correlations among the relaxation ratio, load ratio and calm ratio that are defined as follows (Sagar and Prasad 2012):

$$Relaxation\ ratio = \frac{Average\ energy\ during\ unloading\ phase}{Average\ energy\ during\ loading\ phase}$$

$$Load\ ratio = \frac{Load\ at\ the\ onset\ of\ AE\ activity\ in\ the\ subsequent\ loading}{The\ previous\ maximum\ load}$$

$$Calm\ ratio = \frac{The\ number\ of\ cumulative\ AE\ activities\ during\ unloading\ process}{Total\ AE\ activity\ during\ the\ last\ loading\ cycle\ up\ to\ maximum}$$

Three types of beam samples with different depths 150, 300 and 450 mm were tested. The results showed that the *AE* activities can be affected by the number of cycles. In addition, *AE* energy recorded increased with beam depth (Sagar and Prasad 2012).

Furthermore, the relaxation ratio increased as damage with the cycle number augmented. In other word, the relaxation phase depended upon the level of damage. While the level of damage is trivial, the ratio stays in the loading phase but it comes in the relaxation phase when the level of damage is significant. Besides, by increasing the strain, the damage levels changed from minor to major levels (Sagar and Prasad 2012).

Other researchers studied AE activities on three types of woven carbon/carbon composites having variations during the manufacturing procedure affecting their fiber/matrix interface. They used tensile loading in a load-unload-reload configuration. Four different classes during loading sequence were identified for all types of materials as: Class 1 (matrix cracking), Class 2 (debonding of fiber-matrix and fiber pull-out), Class 3 (thermal stress release, early arrangement of the reinforcement to the loading direction and matrix friction and fiber push-in), and Class 4 (single fibers and fiber bunches failure) (Loutas and Kostopoulos 2009).

5. Structures monitoring

Acoustic emission technique has been established to monitor civil and mine structures because of its capability to sense and localize cracks, quantity their intensity, and assess of level of damage (Grosse and Ohtsu 2008). It has been reported that AET can be successfully applied to predict the damage evolution in reinforced concrete and in historical masonry buildings (Carpinteri and Lacidogna 2003). The cumulative number of counts and released strain energy during cracks propagation in structural members can be used as an approximation at early stages of failure (Carpinteri *et al*. 2007).

The failure mechanism and damage evolution in the masonry composite is significantly intricate. There are several reports related to time-dependent deformations resulted in historic masonry structures collapses (Carpinteri *et al*. 2007, Livitsanos *et al*. 2018).

Researchers have previously monitored two masonry buildings (Casa Capello and Torre Sineo) and revealed that it is possible to estimate the time to final collapse for structures affected by non-concentrated damage by monitoring of damage evolution through AET. Thus, the

possibility of determining the stability or instability of structures can be characterized by the growth of disconnected cracks (Carpinteri *et al*. 2007).

Moreover, Golaski *et al*. (2002) reported their investigation on five different full scale bridges during regular traffic: reinforced concrete, pre-stressed concrete (post-tensioned and pre-tensioned) and combined concrete-steel construction. They introduced the severity parameter (*Sr*) defined as the average signal strength for the 50 events having the major numerical value of signal strength

$$S_r = \frac{1}{50}\sum_{i=1}^{i=50} S_{Oi} \tag{10}$$

where S_r is severity and S_{Oi} is the signal strength of the *i*-th event.

Based on this parameter, they could represented a new way of data analysis in the field of full scale concrete elements or structures evaluating by *AET*. They depicted their results as graphs, which were divided into *A*, *B*, *C*, *D*, and *E* regions. It was concluded that up to 40% of the failure load (region *A*) there were no serious weakening within monitored zones. In the region *B*, small scale cracking and a number of tiny cracks can be detected when the load surpasses 60% of the beam loading capacity. At region *C*, important defect happens and needs more accurate evaluation. Finally at failure regions (*D* and *E*), the tensile crack could be sensed at the side surfaces; however, no fracture of reinforcing was detected (Golaski *et al*. 2002).

Furthermore, there are appropriate reports on the monitoring borehole wall fracture and information in real-time failure (Agioutantis *et al*. 2016, Sarhosis *et al*. 2016). Also, the hydraulic fracturing near the bore hole was simulated. To this end, both the monitoring of borehole wall strain and acoustic emission were used. This combination could provide an effective decision near the borehole subjected to hydraulic fracturing about the classification of fracture initiation and instability mechanism. With respect to borehole wall strain and *AE* events, the fracture process can be categorized into four steps as follows (Liang *et al*. 2017):

1. Micro-crack formation: energy release and *AE* event were not observed.
2. Fracture initiation: in this step the borehole is entirely occupied by water and strain showed a good association with water pressure. Thus, the accumulative and released energy resulting to the creation of areas with intense *AE* were observed.
3. Unstable crack growth: rapid propagation of flaws through fluctuated strain can be sensed in this step. Also, a continuous growing energy leading to the incident of a large number of *AE* events was clear.
4. Fracture closure: no more water was injected in this step. No *AE* events and releasing of energy were reported.

6. Conclusions

The use of Acoustic Emission (*AE*) technique in materials has gained considerable prominence because of the requirements of more durable constructions and health monitoring of structures in future. From this literature review the following conclusions can be made:

In the case of brittle materials, *AE* technique could be applied effectively since the fracture energy is released rapidly and converted to acoustic energy because of brittle nature of materials. However, a plastic component in the material behavior makes the structures more practical and predictable.

It was concluded that the AE technique can successfully be employed for the identification of failure modes giving a comprehensive understanding for a more durable design of structures.

Different modes of fracture expose different *AE* events that vary in terms of frequency, duration and rise time. It has been observed that shear micro-cracks resulted in lower frequency and longer waveforms in average for shear fracture.

Localization of *AE* events could provide appropriate information on the timing and locations of failure.

In the case of stable and unstable crack propagation, the high peak amplitude *AE* hits and the growth of unstable cracks showed a decent correlation.

Rock brittleness has a strong impact on fracture density and *b*-value. An increase in rock brittleness rises the frequency of induced cracks, and proportion of micro- to macro-crack density drops with increasing rock brittleness.

Particle size heterogeneity influences on the number of induced fractures so that under loading, extra fractures were induced in coarse-grained specimens compared to fine-grained ones.

Inducing micro-crack by heating can vary the mode of fractures in specimens from tensile cracks to shear ones, and with increasing of the micro-crack density, the ratio of the number of shear cracks to the number of tensile cracks increases.

Analyses of *AE* parameters indicated that the addition of nano-silica particles has a significant impact on the behavior of micro cracks and failure mechanism of cement mortars.

In the case of fiber reinforced concrete, when the main failure mechanism changes from tensile micro-cracking to macro-cracking with fiber pull out, a severe move in average frequency can be sensed.

Applying of continuous *AE* monitoring during a loading sequence and then analyzing the *AE* events can depict a probable pattern of damage mechanisms and their evolution in different time spans.

In reinforced beams as the strain in steel and concrete increases, the level of damage shifts from minor to major level.

The effect of water can be noticeable in the detected of *AE* events. The reduction in the stress thresholds for crack nucleation, and crack damage occurred by increasing water content in concrete.

References

Aggelis, D.G. (2011), "Classification of cracking mode in concrete

by acoustic emission parameters", *Mech. Res. Commun.*, **38**(3), 153-157. https://doi.org/10.1016/j.mechrescom.2011.03.007.

Aggelis, D.G., Soulioti, D.V., Sapouridis, N., Barkoula, N.M., Paipetis, A.S. and Matikas, T.E. (2011), "Acoustic emission characterization of the fracture process in fibre reinforced concrete", *Constr. Build. Mater.*, **25**(11), 4126-4131. https://doi.org/10.1016/j.conbuildmat.2011.04.049.

Agioutantis Z, Kaklis K, Mavrigiannakis S, Verigakis M, Vallianatos F and Saltas V. (2016), "Potential of acoustic emissions from three point bending tests as rock failure precursors", *Int. J. Min. Sci. Technol.*, **26**(1), 155-160. https://doi.org/10.1016/j.ijmst.2015.11.024.

ASTM International Committee E08 on Fatigue and Fracture. Subcommittee E08. 07 on Fracture Mechanics (2013), Standard Test Method for Linear-elastic Plane-strain Fracture Toughness K_{Ic} of Metallic Materials, ASTM International.

Atkinson, C., Smelser, R.E. and Sanchez, J. (1982), "Combined mode fracture via the cracked Brazilian disk test", *Int. J. Fract.*, **18**(4), 279-291. https://doi.org/10.1007/BF00015688.

Blake ,W. (1972), "Rock-burst mechanics", *Q. Colo. Sch. Mines*, **67**(1), USA.

Blake, W. and Leighton, F. (1969), "Recent developments and applications of the microseismic method in deep mines", *The 11th US Symposium on Rock Mechanics (USRMS)*, American Rock Mechanics Association, Jananuary.

Brühwiler, E. and Wittmann, F.H. (1990), "The wedge splitting test, a new method of performing stable fracture mechanics tests", *Eng. Fract. Mech.*, **35**(1-3), 117-125. https://doi.org/10.1016/0013-7944(90)90189-N.

Carpinteri, A. and Lacidogna, G. (2003), "Damage diagnostic in concrete and masonry structures by acoustic emission technique", *Facta Universitatis-Ser.: Mech. Autom. Control Robot.*, **3**(13), 755-764.

Carpinteri, A. and Shah, S. (2014), *Fracture Mechanics Test Methods for Concrete*, CRC Press.

Carpinteri, A., Lacidogna, G. and Pugno, N. (2007), "Structural damage diagnosis and life-time assessment by acoustic emission monitoring", *Eng. Fract.*, **74**(1-2), 273-289. https://doi.org/10.1016/j.engfracmech.2006.01.036.

Chakrabarti, B.K. and Benguigui, L.G. (1997), *Statistical Physics of Fracture and Breakdown in Disordered Systems*, Oxford University Press.

Dzaye, E.D., De Schutter, G. and Aggelis, D.G. (2018), "Study on mechanical acoustic emission sources in fresh concrete", *Arch. Civil Mech. Eng.*, **18**(3), 742-754. https://doi.org/10.1016/j.acme.2017.12.004.

Elaqra, H., Godin, N., Peix, G., R'Mili, M. and Fantozzi. G. (2007), "Damage evolution analysis in mortar, during compressive loading using acoustic emission and X-ray tomography: effects of the sand/cement ratio", *Cement Concrete Res.*, **37**(5), 703-713. https://doi.org/10.1016/j.cemconres.2007.02.008.

Fowell, R.J., Hudson, J.A., Xu, C. and Zhao, X. (1995), "Suggested method for determining mode I fracture toughness using cracked chevron notched Brazilian disc (CCNBD) specimens", *Int. J. Rock Mech. Min. Sci. Geomech.*, **7**(32), 322.

Franklin, J.A., Zongqi, S., Atkinson, B.K., Meredith, P.C., Rummel, F., Mueller, W., Nishimatsu, Y., Takahahsi, H., Costin, L.S., Ingraffea, A.R. and Bobrov, G.F. (1988), "Suggested methods for determining the fracture toughness of rock", *Int. J. Rock Mech. Min. Geomech.*, **25**(2), 00487481.

Ghazvinian, A., Nejati, H.R., Sarfarazi, V. and Hadei, M.R. (2013), "Mixed mode crack propagation in low brittle rock-like materials", *Arab. J. Geosci.*, **6**(11), 4435-4444. https://doi.org/10.1007/s12517-012-0681-8.

Golaski, L., Gebski, P. and Ono, K. (2002), "Diagnostics of reinforced concrete bridges by acoustic emission", *J. Acoust. Emission.*, **20**, 83-89.

Grégoire, D., Verdon, L., Lefort, V., Grassl, P., Saliba, J., Regoin, J.P., Loukili, A. and Pijaudier-Cabot, G. (2015), "Mesoscale analysis of failure in quasi-brittle materials: comparison between lattice model and acoustic emission data", *Int. J. Numer. Anal. Meth. Geomech.*, **39**(15), 1639-1664. https://doi.org/10.1002/nag.2363.

Grosse, C.U. and Ohtsu, M. (2008), *Acoustic Emission Testing*, Springer Science & Business Media.

Gutenberg B. (2013), *Seismicity of the Earth and Associated Phenomena*, Read Books Ltd.

Hadigheh, S.A., Gravina, R.J. and Smith, S.T. (2017), "Effect of acid attack on FRP-to-concrete bonded interfaces", *Constr. Build. Mater.*, **152**, 285-303. https://doi.org/10.1016/j.conbuildmat.2017.06.140.

Haidar, K., Pijaudier-Cabot, G., Dubé, J.F. and Loukili, A. (2005), "Correlation between the internal length, the fracture process zone and size effect in model materials", *Mater. Struct.*, **38**(2), 201. https://doi.org/10.1007 / BF02479345.

Hall, S.A., De Sanctis, F. and Viggiani, G. (2006), "Monitoring fracture propagation in a soft rock (Neapolitan Tuff) using acoustic emissions and digital images", *Pure Appl. Geophys.*, **163**(10), 2171-2204. https://doi.org/10.1007/s00024-006-0117-z.

Haneef, T.K., Kumari, K., Mukhopadhyay, C.K., Rao, B.P. and Jayakumar, T. (2013), "Influence of fly ash and curing on cracking behavior of concrete by acoustic emission technique", *Constr. Build. Mater.*, **44**, 342-350. https://doi.org/10.1016/j.conbuildmat.2013.03.041.

Haneef, T.K., Mukhopadhyay, C.K., Rao, B.P. and Jayakumar, T. (2010), "Acoustic emissions generated during Lüders band elongation of tempered medium carbon steel", *Streng. Fract. Complex.*, **6**(4), 149-159. https://doi.org/10.3233/SFC-2011-0113.

Imani, M., Nejati, H.R. and Goshtasbi, K. (2017), "Dynamic response and failure mechanism of Brazilian disk specimens at high strain rate", *Soil Dyn. Earthq. Eng.*, **100**, 261-269. https://doi.org/10.1016/j.soildyn.2017.06.007.

Irwin, G.R. (1957), "Analysis of stresses and strains near the end of a crack traversing a plate", *J. Appl. Mech.*

JCMS-III B5706 (2003), Monitoring Mmethod for Active Cracks in Concrete by Acoustic Emission, Federation of Construction Materials Industries, Japan.

Kaiser, J. (1950), "An investigation into the occurrence of noises in tensile tests, or a study of acoustic phenomena in tensile tests", PhD Thesis.

Kawasaki, Y., Kitaura, M., Kobarai, T. and Ohtsu, M. (2011), "Corrosion damage in reinforced concrete identified by AE", *Concrete Res. Lett.*, **2**(3), 262-266.

Kawasaki, Y., Okamoto, T. and Izuno, K. (2015), "Corrosion-induced cracks in concrete and hybrid non-destructive evaluation (NDE) for evaluation in rebar corrosion", *Acoustic Emission and Related Non-Destructive Evaluation Techniques in the Fracture Mechanics of Concrete*.

Khodayar, A. and Nejati, H.R. (2018), "Effect of thermal-induced microcracks on the failure mechanism of rock specimens", *Comput. Concrete*, **22**(1), 93-100. https://doi.org/10.12989/cac.2018.22.1.093.

Köppel, S. and Grosse, C. (2000), "Advanced acoustic emission techniques for failure analysis in concrete", *WCNDT Proceedings*.

Kumar, S. and Barai, S.V. (2011), *Concrete Fracture Models and Applications*, Springer Science & Business Media.

Kurz, J.H., Finck, F., Grosse, C.U. and Reinhardt, H.W. (2006), "Stress drop and stress redistribution in concrete quantified over time by the b-value analysis", *Struct. Hlth. Monit.*, **5**(1), 69-81. https://doi.org/10.1177/1475921706057983.

Kurz, J.H., Grosse, C.U. and Reinhardt, H.W. (2005), "Strategies for reliable automatic onset time picking of acoustic emissions and of ultrasound signals in concrete", *Ultrasonic.*, **43**(7), 538-546. https://doi.org/10.1016/j.ultras.2004.12.005.

L'Hermite, R.G. (1960), "Volume changes of concrete", *Proceedings of the 4th Int. Symposium on the Chemistry of Cement*, 659.

Lavrov, A. (2003), "The Kaiser effect in rocks: principles and stress estimation techniques", *Int. J. Rock Mech. Min. Sci.*, **40**(2), 151-171. https://doi.org/10.1016/S1365-1609(02)00138-7.

Liang, Y., Cheng, Y., Zou, Q., Wang, W., Ma, Y. and Li, Q. (2017), "Response characteristics of coal subjected to hydraulic fracturing: An evaluation based on real-time monitoring of borehole strain and acoustic emission", *J. Natur. Gas Sci. Eng.*, **38**, 402-411. https://doi.org/10.1016/j.jngse.2017.01.001.

Livitsanos, G., Shetty, N., Hündgen, D., Verstrynge, E., Wevers, M., Van Hemelrijck, D. and Aggelis, D.G. (2018), "Acoustic emission characteristics of fracture modes in masonry materials", *Constr. Build. Mater.*, **162**, 914-922. https://doi.org/10.1016/j.conbuildmat.2018.01.066.

Loutas, T.H. and Kostopoulos, V. (2009), "Health monitoring of carbon/carbon, woven reinforced composites. Damage assessment by using advanced signal processing techniques. Part I: Acoustic emission monitoring and damage mechanisms evolution", *Compos. Sci. Technol.*, **69**(2), 265-272. https://doi.org/10.1016/j.compscitech.2008.07.020.

Mihashi, H., Nomura, N. and Niiseki, S. (1991), "Influence of aggregate size on fracture process zone of concrete detected with three dimensional acoustic emission technique", *Cement Concrete Res.*, **21**(5), 737-744. https://doi.org/10.1016/0008-8846(91)90168-H.

Mukhopadhyay, C.K., Rajkumar, K.V., Jayakumar, T. and Raj, B. (2010), "Study of tensile deformation behaviour of M250 grade maraging steel using acoustic emission", *J. Mater. Sci.*, **45**(5), 1371-1384. https://doi.org/10.1007/s10853-009-4095-2.

Najigivi, A., Nazerigivi, A. and Nejati, H.R. (2017), "Contribution of steel fiber as reinforcement to the properties of cement-based concrete: a review", *Comput. Concrete*, **20**(2), 155-164. https://doi.org/10.12989/cac.2017.20.2.155.

Nazerigivi, A. and Najigivi, A. (2019), "Study on mechanical properties of ternary blended concrete containing two different sizes of nano-SiO_2", *Compos. Part B: Eng.*, **167**, 20-24. https://doi.org/10.1016/j.compositesb.2018.11.136.

Nazerigivi, A., Nejati, H.R., Ghazvinian, A. and Najigivi, A. (2018), "Effects of SiO_2 nanoparticles dispersion on concrete fracture toughness", *Constr. Build. Mater.*, **171**, 672-679. https://doi.org/10.1016/j.conbuildmat.2018.03.224.

Nazerigivi, A., Nejati, H.R., Ghazvinian, A. and Najigivi, A. (2017), "Influence of nano-silica on the failure mechanism of concrete specimens", *Comput. Concrete*, **19**(4), 429-434. https://doi.org/10.12989/cac.2017.19.4.429.

Nejati, H.R. and Ghazvinian, A. (2014), "Brittleness effect on rock fatigue damage evolution", *Rock Mech. Rock Eng.*, **47**(5), 1839-1848. https://doi.org/10.1007/s00603-013-0486-4.

Ohno, K. (2015), "Identification of the fracture process zone in concrete materials by acoustic emission", *Acoustic Emission and Related Non-Destructive Evaluation Techniques in the Fracture Mechanics of Concrete*.

Ohtsu, M. (1998), "Basics of acoustic emission and applications to concrete engineering", *J. Soc. Mater. Sci.*, **47**(9), 131-140. https://doi.org/10.2472/jsms.47.9Appendix_131.

Ohtsu, M. (2015), *Acoustic Emission and Related Non-Destructive Evaluation Techniques in the Fracture Mechanics of Concrete: Fundamentals and Applications*, Woodhead Publishing.

Ohtsu, M., Mori, K. and Kawasaki, Y. (2011), "Corrosion process and mechanisms of corrosion-induced cracks in reinforced concrete identified by AE analysis", *Strain*, **47**, 179-186. https://doi.org/10.1111/j.1475-1305.2010.00754.x.

Raj, B. and Jayakumar, T. (1991), "Acoustic emission during tensile deformation and fracture in austenitic alloys", *Acoustic Emission: Current Practice and Future Directions*, ASTM International.

Ranjith, P.G., Jasinge, D., Song, J.Y. and Choi, S.K. (2008), "A study of the effect of displacement rate and moisture content on the mechanical properties of concrete: use of acoustic emission", *Mech. Mater.*, **40**(6), 453-469. https://doi.org/10.1016/j.mechmat.2007.11.002.

Recommendation, R.D. (1985), "Determination of the fracture energy of mortar and concrete by means of three-point bend tests on notched beams", *Mater. Struct.*, **18**(106), 285-290.

Reis, J.M., De Oliveira, R., Ferreira, A.J. and Marques, A.T. (2003), "A NDT assessment of fracture mechanics properties of fiber reinforced polymer concrete", *Polym. Test.*, **22**(4), 395-401. https://doi.org/10.1016/S0142-9418(02)00120-4.

Ren, X., Chen, J.S., Li, J., Slawson, T.R. and Roth, M.J. (2011), "Micro-cracks informed damage models for brittle solids", *Int. J. Solid. Struct.*, **48**(10), 1560-1571. https://doi.org/10.1016/j.ijsolstr.2011.02.001.

Robinson, G.S. (1965), "Methods of detecting the formation and propagation of microcracks in concrete", *Proceedings of the Int. Conference on the Structure of Concrete and its Behavior under Load, Cement and Concrete Association*, 131-145.

Rüsch, H. (1960), "Physical problems in the testing of concrete", *Cement and Concrete Association*.

Sabri, M., Ghazvinian, A. and Nejati, H.R. (2016), "Effect of particle size heterogeneity on fracture toughness and failure mechanism of rocks", *Int. J. Rock Mech. Min. Sci.*, **81**, 79-85. https://doi.org/10.1016/j.ijrmms.2015.11.002.

Sagar, R.V. and Prasad, B.R. (2012), "Damage limit states of reinforced concrete beams subjected to incremental cyclic loading using relaxation ratio analysis of AE parameters", *Constr. Build. Mater.*, **35**, 139-148. https://doi.org/10.1016/j.conbuildmat.2012.02.057.

Sarhosis, V., Jaya, A.A. and Thomas, H.R. (2016), "Economic modelling for coal bed methane production and electricity generation from deep virgin coal seams", *Energy*, **107**, 580-594. https://doi.org/10.1016/j.energy.2016.04.056.

Sellers, E.J., Kataka, M.O. and Linzer, L.M. (2003), "Source parameters of acoustic emission events and scaling with mining-induced seismicity", *J. Geophys. Res.: Solid Earth*, **108**(B9). https://doi.org/10.1029/2001JB000670.

Shiotani, T., Ohtsu, M. and Ikeda, K. (2001), "Detection and evaluation of AE waves due to rock deformation", *Constr. Build. Mater.*, **15**(5-6), 235-246. https://doi.org/10.1016/S0950-0618(00)00073-8.

Soulioti, D., Barkoula, N.M., Paipetis, A., Matikas, T.E., Shiotani, T. and Aggelis, D.G. (2009), "Acoustic emission behavior of steel fibre reinforced concrete under bending", *Constr. Build. Mater.*, **23**(12), 3532-3536. https://doi.org/10.1016/j.conbuildmat.2009.06.042.

Suzuki, T., Shiotani, T. and Ohtsu, M. (2017), "Evaluation of cracking damage in freeze-thawed concrete using acoustic emission and X-ray CT image", *Constr. Build. Mater.*, **136**, 619-626. https://doi.org/10.1016/j.conbuildmat.2016.09.013.

Szendi-Horvath, G. (1982), "On fracture toughness of coal", *Aust. J. Coal Min. Technol.*, **2**, 51-57.

Watanabe, T., Nishibata, S., Hashimoto, C. and Ohtsu, M. (2007), "Compressive failure in concrete of recycled aggregate by acoustic emission", *Constr. Build. Mater.*, **21**(3), 470-476. https://doi.org/10.1016/j.conbuildmat.2006.04.002.

Whittaker, B.N., Singh, R.N. and Sun, G. (1992), *Rock Fracture Mechanics Principles, Design and Applications, Developments in Geotechnical Engineering*, Elsevier Publishers, Netherlands.

Wittmann, F.H. (1986), *Fracture Toughness and Fracture Energy of Concrete*, Elsevier.

Wu, K., Chen, B. and Yao, W. (2001), "Study of the influence of aggregate size distribution on mechanical properties of concrete by acoustic emission technique", *Cement Concrete Res.*, **31**(6), 919-23. https://doi.org/10.1016/S0008-8846(01)00504-X.

Zang, A., Christian Wagner, F., Stanchits, S., Dresen, G., Andresen, R. and Haidekker, M.A. (1998), "Source analysis of acoustic emissions in Aue granite cores under symmetric and asymmetric compressive loads", *Geophys. J. Int.*, **135**(3), 1113-1130. https://doi.org/10.1046/j.1365-246X.1998.00706.x.

Zhang, P., Dai, X.B., Gao, J.X. and Wang, P. (2015), "Effect of nano-SiO_2 particles on fracture properties of concrete composite containing fly ash", *Curr. Sci.*, **108**(11), 2035-2043.

Zhang, P., Gao, J.X., Dai, X.B., Zhang, T.H. and Wang, J. (2016), "Fracture behavior of fly ash concrete containing silica fume", *Struct. Eng. Mech.*, **59**(2), 261-275. https://doi.org/10.12989/sem.2016.59.2.261.

Zhang, P., Liu, C.H., Li, Q.F. and Zhang, T.H. (2013), "Effect of polypropylene fiber on fracture properties of cement treated crushed rock", *Compos. Part B: Eng.*, **55**, 48-54. https://doi.org/10.1016/j.compositesb.2013.06.005.

CC